Human cone photoreceptor dependence on RPE65 isomerase

Samuel G. Jacobson*†, Tomas S. Aleman*, Artur V. Cideciyan*, Elise Heon‡, Marcin Golczak§, William A. Beltran¶, Alexander Sumaroka*, Sharon B. Schwartz*, Alejandro J. Roman*, Elizabeth A. M. Windsor*, James M. Wilson‖, Gustavo D. Aguirre¶, Edwin M. Stone**, and Krzysztof Palczewski†§

*Scheie Eye Institute, Department of Ophthalmology, School of Medicine, ¶Section of Ophthalmology, School of Veterinary Medicine, and ‖Department of Pathology and Laboratory Medicine, University of Pennsylvania, Philadelphia, PA 19104; ‡Department of Ophthalmology and Vision Sciences, The Hospital for Sick Children, University of Toronto, Toronto, ON, Canada M56 1X8; §Department of Pharmacology, Case Western Reserve University, Cleveland, OH 44106; and **Department of Ophthalmology, University of Iowa Carver College of Medicine, Iowa City, IA 52242

Edited by Jeremy Nathans, Johns Hopkins University School of Medicine, Baltimore, MD, and approved August 3, 2007 (received for review July 6, 2007)

The visual (retinoid) cycle, the enzymatic pathway that regenerates chromophore after light absorption, is located primarily in the retinal pigment epithelium (RPE) and is essential for rod photoreceptor survival. Whether this pathway also is essential for cone photoreceptor survival is unknown, and there are no data from man or monkey to address this question. The visual cycle is naturally disrupted in humans with Leber congenital amaurosis (LCA), which is caused by mutations in *RPE65*, the gene that encodes the retinoid isomerase. We investigated such patients over a wide age range (3–52 years) for effects on the cone-rich human fovea. *In vivo* microscopy of the fovea showed that, even at the youngest ages, patients with *RPE65*-LCA exhibited cone photoreceptor loss. This loss was incomplete, however, and residual cone photoreceptor structure and function persisted for decades. Basic questions about localization of RPE65 and isomerase activity in the primate eye were addressed by examining normal macaque. RPE65 was definitively localized by immunocytochemistry to the central RPE and, by immunoblotting, appeared to concentrate in the central retina. The central retinal RPE layer also showed a 4-fold higher retinoid isomerase activity than more peripheral RPE. Early cone photoreceptor losses in *RPE65*-LCA suggest that robust RPE65-based visual chromophore production is important for cones; the residual retained cone structure and function support the speculation that alternative pathways are critical for cone photoreceptor survival.

optical coherence tomography | retinal degeneration | retinoid cycle | Leber congenital amaurosis | gene therapy

Vertebrate retinas have two types of photoreceptors: rods for the perception of dim light and cones for the perception of bright light. Light absorbed by visual pigments of photoreceptors triggers a series of enzymatic reactions known as phototransduction (1). The light-capturing part of the visual pigment, the chromophore, must then be regenerated. The pathway for regeneration of rhodopsin (the rod visual pigment) is known as the visual (retinoid) cycle (2, 3) and involves both rod cells and the adjacent retinal pigment epithelium (RPE). *All-trans*-retinal is reisomerized to 11-*cis*-retinal by a reaction in the RPE that requires the retinal isomerase, retinal pigment epithelium-specific 65-kDa protein (RPE65), and lecithin–retinol acyltransferase (LRAT) activities. Functional visual pigment is then reformed by combining the 11-*cis*-chromophore with the photoreceptor opsin apoprotein (4). Molecular knowledge of the visual cycle has increased as the genes encoding the enzymes of this pathway have been elucidated (2, 5, 6).

Decades ago, cone pigment regeneration was proposed to be RPE cell-independent (7, 8). More recently, cone-dominant ground squirrel and chicken retinas have been shown to exhibit retinoid isomerase activity that is distinct from RPE65 (5, 9, 10). Murine double knockout experiments, however, provide evidence that RPE65 and the RPE are essential for cone function (11). Further complexity has been added by immunohistochemical evidence of RPE65 protein in cone photoreceptors of retinas from salamanders and mammals, including mouse, rabbit, and cow (12); both short-wavelength (SW) and long-wavelength (LW) murine cones were RPE65-positive. At variance, however, are other reports that failed to identify RPE65 immunoreactivity in cone photoreceptors of cow, rat, chicken, frog, $Nrl^{-/-}$ mice (11, 13), dogs (14), and human extrafoveal retina (13).

To gain insight into human cone visual pigment regeneration, we used an experimental paradigm common in studies of genetically engineered or naturally occurring mutant animals. Selective disruption of the retinoid isomerase, RPE65, occurs in humans with the eye disease known as Leber congenital amaurosis (LCA) (6, 15–19). Human and nonhuman primate eyes have a cone-rich fovea (20, 21), which is a unique retinal topographical feature that enables the study of cone-specific properties and mechanisms. We found that RPE65-deficient patients over a wide age range showed early loss of foveal photoreceptors, indicating that RPE65 is important for cone photoreceptor function and survival, yet there also was residual decades-long persistence of foveal cones in *RPE65*-LCA, which raises questions about the mechanisms responsible for cone survival. We investigated the localization of RPE65 and isomerase activities in primates by using normal monkey eyes. The results have strong clinical implications because of ongoing human clinical trials of somatic gene therapy that seek to restore useful central vision to *RPE65*-LCA patients (22–24).

Results

Isomerase-Deficient Human Retina in *RPE65*-LCA Showed Early Cone Photoreceptor Loss. The fovea is the location of peak cone photoreceptor density, and a steep decline of cone density occurs with increasing eccentricity from the foveal center (20). The foveal landmark can be identified by *in vivo* cross-sectional imaging of the human central retina, providing the opportunity to quantify cone photoreceptor layer thickness (22). Scans across the horizontal and vertical meridians of a 12-year-old normal subject illustrate the foveal depression and adjacent laminar architecture (Fig. 1*A*). The deep layer (highlighted in blue) that peaks in thickness at the fovea is the photoreceptor or outer nuclear layer (ONL). Representative

Author contributions: S.G.J., T.S.A., A.V.C., E.H., M.G., W.A.B., A.S., J.M.W., G.D.A., E.M.S., and K.P. designed research; S.G.J., T.S.A., A.V.C., E.H., M.G., W.A.B., A.S., S.B.S., A.J.R., E.A.M.W., and K.P. performed research; S.G.J., T.S.A., A.V.C., M.G., W.A.B., A.S., S.B.S., A.J.R., E.A.M.W., J.M.W., G.D.A., E.M.S., and K.P. analyzed data; and S.G.J., T.S.A., A.V.C., and K.P. wrote the paper.

The authors declare no conflict of interest.

This article is a PNAS Direct Submission.

Abbreviations: LCA, Leber congenital amaurosis; LW, long wavelength; MAR, minimal angle of resolution; OCT, optical coherence tomography; ONL, outer nuclear layer; RPE, retinal pigment epithelium; sRBI, subRPE backscattering index; SW, short wavelength.

†To whom correspondence may be addressed. E-mail: jacobsos@mail.med.upenn.edu or kxp65@case.edu.

This article contains supporting information online at www.pnas.org/cgi/content/full/0706367104/DC1.

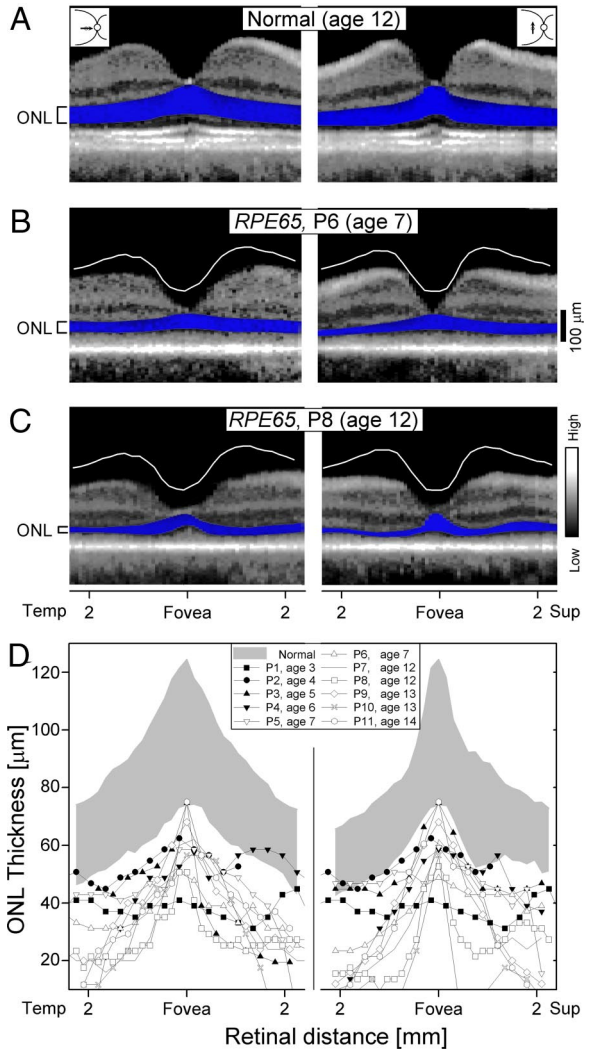

Fig. 1. Photoreceptor layer thickness in the central retinas of a normal child and two children with *RPE65*-LCA. (*A–C*) Horizontal and vertical OCT scans with the ONL highlighted in blue and labeled on the left. In the scans from P6 and P8, the white line indicates the lower limit of normal retinal thickness. (*D*) ONL thickness along the horizontal and vertical meridians in *RPE65*-LCA patients (n = 11; ages 3–14 years). Data from P7 (line without symbols) have been previously published (22). Gray regions represent normal limits (mean ± 2 SD; n = 10; ages 4–16 years). Temp, temporal; Sup, superior.

scans from two young patients with *RPE65*-LCA show abnormalities in retinal structure (Fig. 1 *B* and *C*). P6, a 7-year-old girl, had normal-appearing laminar architecture, but the central retina was abnormally thin. ONL thickness was subnormal in the central 4 mm. The vertical scan also showed reduced central thickness. P8, at age 12, also had retinal and ONL thinning across the scanned regions, including the fovea.

ONL thickness was analyzed across the horizontal and vertical meridians in normal subjects (n = 10; ages 4–16 years) and in young *RPE65*-LCA patients (n = 11; ages 3–14 years) (Fig. 1*D* and Table 1). Foveal photoreceptor layer peak thickness was decreased, reaching the lower limit of normal in only two (ages 5 and 14) of the 11 patients studied. Slightly eccentric to the fovea, however, all patients had abnormally reduced ONL thicknesses. At further eccentricities, many patients showed major ONL reductions, whereas others maintained a detectable but reduced ONL.

Some Foveal Cone Photoreceptors Survived for Decades. A comparison of central retinal ONL thickness data in three age groups of

Table 1. Molecular characteristics of *RPE65* patients

Patient	Age at visit, years	Sex	Mutations	Source
Age group 1				
P1[a]	3	M	R91W/R91W	This study
P2[b]	4	M	A500del5bp/ A500del5bp	This study
P3[b]	5	F	A500del5bp/ A500del5bp	This study
P4[c]	6	M	R44Q/R44Q	This study
P5[c]	7	M	R44Q/R44Q	This study
P6[a]	7	F	R91W/R91W	This study
P7	12	F	97del20bp/ 97del20bp	Refs. 22, 56, and 57
P8	12	F	L408P/L408P	This study
P9	13	M	Y368H/Y368H	Ref. 22
P10	13	F	V287F/V287F	Ref. 56
P11	14	F	R91Q/R91W	This study
Age group 2				
P12	18	F	L341S/L341S	Ref. 22
P13	19	M	R91W/R91W	Ref. 49
P14	19	F	G40S/R91Q	Ref. 49
P15	21	F	R91W/R44Q	Ref. 22
P16	23	M	E417Q/E417Q	Ref. 22
P17	23	M	R91W/ 1059_1060ins1bp	This study
P18	27	F	H182R/H182R	Ref. 22
P19	28	F	Y368H/ 297del1bp	Ref. 22
Age group 3				
P20	31	F	R91Q/ IVS7 + 4A > G	Ref. 57
P21	40	F	K303X/Y431C	Ref. 22
P22	41	M	Y144D/Y144D	Ref. 22
P23	52	M	IVS1 + 5G > A homoallelic	Refs. 22 and 58

Patients with the same superscipt letter (a, b, and c) are from the same pedigree. The references listed are previous reports of genotype and/or phenotype.

RPE65-LCA patients (Fig. 2 *A–C* and Table 1) revealed little difference on average between foveal peak ONL in group 1 (mean ± SE = 59.4 ± 6.8 μm; 61% of age-matched normal controls) compared with group 2 (mean ± SE = 61.4 ± 12.8 μm; 65% of age-matched controls). However, the ONL loss was greater in group 3 (mean ± SE = 38.4 ± 19.2 μm; 37% of age-matched controls). These grouped data suggest that partial loss of cones in the central retina is present from early childhood, and residual cones may decline slowly over decades. Amounts of residual foveal cone structure in *RPE65*-LCA varied. This result was apparent at all ages when the average ONL thickness in the foveal region was plotted as a function of age and compared with the normal controls (Fig. 2*D*). Consistent with the results from grouped data, the average foveal ONL was abnormally reduced for every individual patient, compared with the 95% prediction interval of results in normal controls (Fig. 2*D*). Linear regression fit to the patient results suggested a 5.3-μm thinning per decade, whereas normal subjects showed a 1.6-μm thickening per decade.

Foveal RPE Integrity with Partial Cone Loss. We investigated whether RPE pigmentation, a measure of RPE integrity, was retained in the same foveal region that showed partial loss of photoreceptors from early life. The index of RPE pigmentation, the subRPE backscattering index (sRBI), was within normal limits for all group 1 patients and the majority of group 2 patients (Fig. 2*E*). These findings

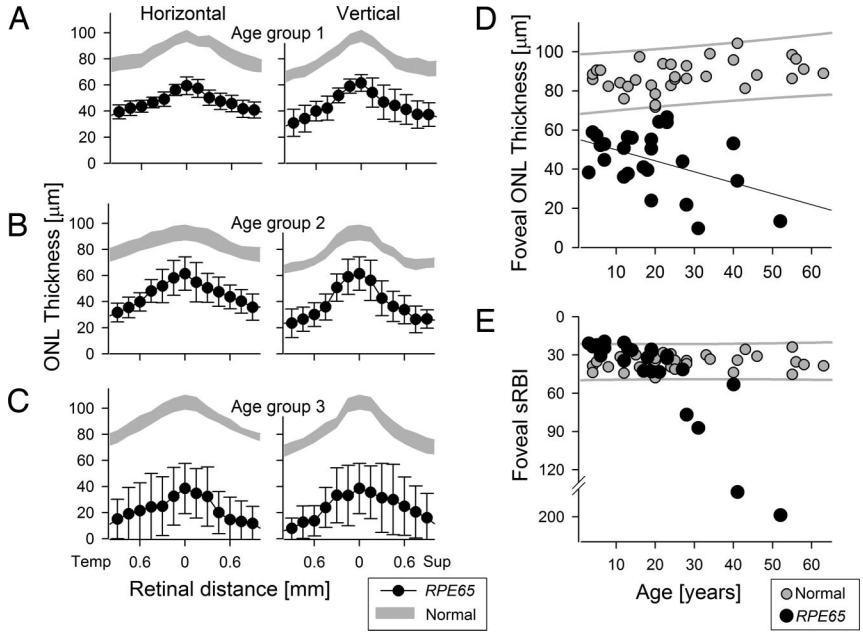

Fig. 2. Prolonged survival of residual central cones after early loss in *RPE65*-LCA patients. (*A–C*) Comparison of mean central ONL thickness along horizontal and vertical meridians in three age groups of *RPE65*-LCA (symbols) and normal (gray regions) individuals. Error bars and the extent of the gray regions represent mean ± 2 SE. Subject ages for *RPE65*-LCA patients/normals were as follows: group 1, 3–14 years/4–16 years; group 2, 18–28 years/19–28 years; group 3, 31–52 years/33–63 years. (*D*) Average ONL thickness of the foveal region (central cross extending to 0.6 mm) as a function of age in patients (black symbols) and normal controls (gray symbols). The 95% prediction interval of linear regression fit to the normal data (gray lines) and linear regression fit to the patient data (black line) are shown. (*E*) Average sRBI of the foveal region as a function of age in patients and normal controls. The 95% prediction interval of linear regression fit to the normal data (gray lines) is shown.

suggest that foveal RPE remains relatively healthy from early life through the third decade, although there is partial loss of cones. Group 3 patients, in contrast, showed various abnormalities in sRBI, suggesting the presence of RPE demelanization and disease with progression of central retinal degeneration.

Residual Cone Function in *RPE65*-LCA Means Chromophore Availability. Psychophysical evidence of residual cone-mediated function in *RPE65*-LCA is illustrated for two young adults (Fig. 3*A*). Dark-adapted sensitivity measurements across the horizontal meridian indicate detectable function that is at least 5 log units less sensitive to light than normal. Chromatic stimuli show a difference in sensitivities between long- and short-wavelength light that is consistent with the spectral sensitivity of LW cones (25). SW cone function assessed in six patients (group 1, two patients; group 2, three patients; group 3, one patient) indicated that none of them had detectable SW cone function.

Visual acuity and fixation stability also were quantified in *RPE65*-LCA individuals. Visual acuity was abnormally reduced but measurable in all patients during the first three decades of life (Fig. 3 *B* and *C*), which is in agreement with a previous report (26). In groups 1 and 2, visual acuity could be as good as 0.3 logMAR, but also could be far more reduced. There was no apparent relationship of visual acuity with age in these groups, but patients studied at ages >28 years showed severe visual acuity losses, and many only had light perception (Fig. 3*B*). Normal visual acuity is mediated at the fovea, where the highest spatial density of cone photoreceptors resides (20, 27). Reduced acuity can relate to a dysfunctional fovea (28, 29) or by the adoption of extrafoveal retina for fixation to compensate for dysfunction or degeneration of foveal cones (30). Correspondence of the center of the anatomical fovea to fixation was evaluated by optical coherence tomography (OCT) in all patients. All but one patient (P19) in groups 1 and 2 fixated at or near the fovea (data not shown) with one eye (right eye of P13 and P18) or both eyes (P3–P12, P14–P17). The majority showed abnormal eye movements during this fixation task, which was clinically manifest in most patients (except P8 and P17) as nystagmus of various degrees. Patients from group 3 exhibited wandering eye movements without a specific locus of fixation. In a subset of eight patients (P9–P11, P13–P17), eye movements were quantified under fundus visualization during fixation to a light stimulus bright enough to be perceptible. Average fixation instability ranged from 0.19° to 0.45° (normal mean ± SD; 0.10 ± 0.06°; $n = 4$) and was linearly related to logMAR visual acuity (Fig. 3*C*). In summary, *RPE65*-LCA patients exhibited detectable LW cone-mediated function and used the LW cone-rich central retina at or near the fovea for fixation and letter discrimination tasks.

Isomerase Was Detected Only in Primate RPE, and Isomerization Activity in the Central Retina Exceeded That in the Peripheral Retina. Whether RPE65 protein is detectable in mammalian and human photoreceptors is controversial (12, 13). To clarify this issue, we examined the cone-rich monkey fovea (Fig. 4*A*). RPE65 labeling was found to be restricted to RPE cells in the macaque fovea (Fig. 4 *B* and *C*). No RPE65 labeling was detected in foveal SW or LW cones and none in rods. Extrafoveal cones also showed no RPE65 labeling (data not shown).

To investigate potential variations in RPE65-related isomerization activity between the central and peripheral retinas, we examined RPE layers in 5-mm punches in different parts of the macaque eye. Together with higher retinoid amounts, including the fatty acid *all-trans*-retinyl esters [supporting information (SI) Table 2 and SI Fig. 5], the macula had four times the isomerization activity of the periphery as assessed by production of 11-*cis*-retinol (Fig. 4 *D* and *E*). Moreover, this activity strongly correlated with the expression level of RPE65, which was the highest in the macula (Fig. 4*F*). Together these results suggest that the macula has the highest levels of both substrate and enzyme as measured by expression of the key protein, RPE65, and directly in the enzymatic assays. Thus, robust

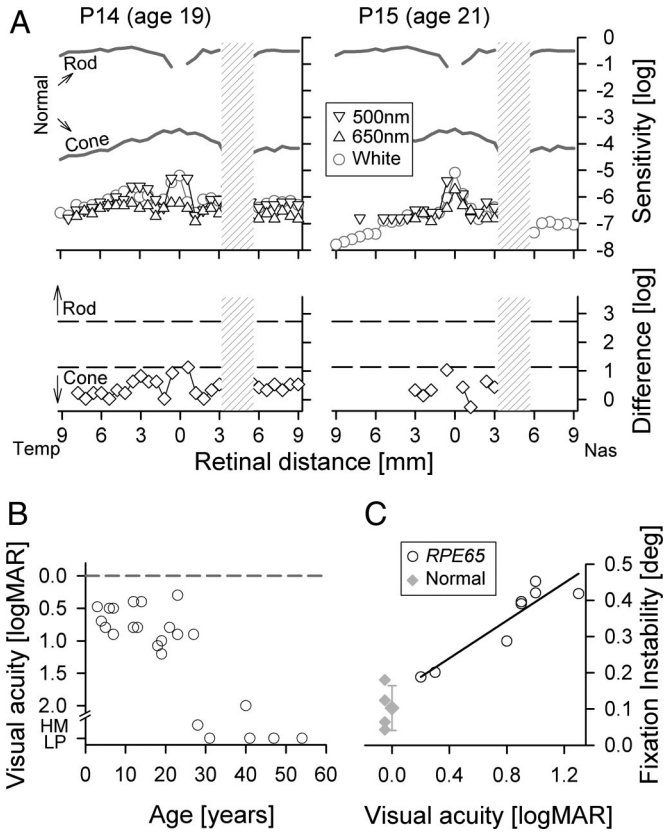

Fig. 3. Persistent cone visual function in *RPE65*-LCA means persistent chromophore availability. (*A*) (*Upper*) Dark-adapted psychophysical sensitivities to chromatic and achromatic stimuli presented across the horizontal meridian in young adult *RPE65*-LCA patients. Sensitivities to chromatic stimuli are shown on a common axis of radiometric equivalence, and sensitivities to achromatic stimuli are vertically shifted to match the blue stimulus results. Mean normal dark-adapted rod sensitivity to 500-nm stimulus and dark-adapted cone sensitivity to 650-nm stimulus during the cone plateau are shown (gray lines). (*Lower*) Comparison of the difference in chromatic sensitivity at each locus (symbols) to predicted difference for rod or cone mediation (dashed lines) based on spectral sensitivities of normal rod- and cone-mediated vision. Physiological blind spot is shown as a hatched bar. Temp, temporal; Nas, nasal. (*B*) Best-corrected visual acuity for the better-seeing eye in patients with *RPE65* mutations, showing the range of function in young patients and worsening of acuity after the third decade of life. HM, hand motions; LP, light perception. Dashed line corresponds to 20/20 (log of the minimal angle of resolution, logMAR, 0.0) acuity. (*C*) Instability of fixation determined under retinal visualization in *RPE65*-LCA as it relates to visual acuity. Normal results are shown (gray symbols); error bars indicate ±SD.

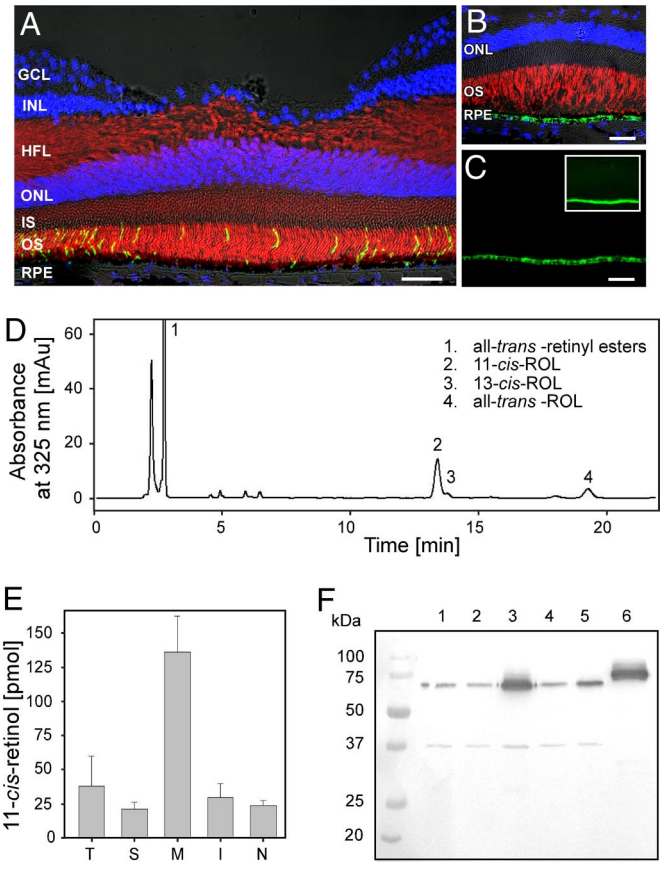

Fig. 4. RPE65 localization and RPE65-dependent isomerase activity and its distribution in the macaque eye. (*A*) Double-fluorescence immunolabeling of foveal rod outer segments (green) and cones (red) with rhodopsin and cone arrestin antibodies, respectively, shows normal lamination of the central retina. RPE, retinal pigment epithelium; IS, inner segments; OS, outer segments; ONL, outer nuclear layer; HFL, Henle's fiber layer; INL, inner nuclear layer; GCL, ganglion cell layer. (*B*) Double-fluorescence immunolabeling of a monkey fovea with RPE65 (green) and R/G opsin (red) antibodies shows no expression of RPE65 in cones. Nuclei were stained with DAPI (blue), and Nomarski differential interference contrast microscopy optics was used. (*C*) Immunolabeling with RPE65 antibody (green) is only seen in the RPE. (*Inset*) Overexposed image does not show any RPE65 labeling in the fovea other than in the RPE. (Scale bars: *A–C*, 40 μm.) (*D*) HPLC separation of nonpolar retinoids extracted from the isomerization reaction mixture. RPE microsomes were isolated from a single eye, and the isomerization reaction was carried out as described in *Materials and Methods*. (*E*) Isomerization activities in different regions of the eye. T, temporal; S, superior; M, macula; I, inferior; N, nasal. (*F*) Immunoblot analysis of RPE65 expression levels in 5-mm biopsy punches taken from different areas of the eye. Lines 1–5 represent RPE microsomes dissected from temporal, superior, macula, inferior, and nasal parts of an eye, respectively. Line 6 is a human recombinant-tagged RPE65 expressed in Sf9 cells.

RPE65-based visual chromophore production must be considered as an important factor in supporting cone function.

Discussion

Conformational shift of 11-*cis*-retinal chromophore upon absorption of a photon is the key event that allows signaling of light in both rod and cone photoreceptors. Although rods require 11-*cis*-retinal produced in the RPE by reactions that necessitate RPE65 and lecithin–retinol acyltransferase (LRAT) activities, regeneration of at least some of the cone pigments has been proposed to originate in the retina (5–10). Cone-dominant animal retinas exhibit a retinoid isomerase activity that converts *all-trans*-retinol directly to its 11-*cis*-retinol isomer, and the reaction is driven by secondary esterification of 11-*cis*-retinol to its ester in a palmitoyl-CoA-dependent reaction (9, 10). Unlike the situation in the RPE, where 11-*cis*-retinol is efficiently oxidized by NADP/NADPH-dependent 11-*cis*-retinol dehydrogenase, a cone-specific pathway implies trapping of 11-*cis*-retinol in the form of esters or bound to cellular retinaldehyde-binding protein (6). Interestingly, we found both 11-*cis*-retinol and its palmitoyl ester to be highly abundant retinoids in the monkey eye (SI Fig. 5), suggesting a different retinoid distribution compared with the rod-dominant rodents. The central retinal region in the monkey eye, which is greatly enriched in cones, also was characterized by the highest RPE-based isomerization activity and RPE65 expression level (Fig. 4). Our immunocytochemical results further strengthened the argument that RPE65 in primates is expressed only in the RPE layer. Of interest, the protein product of another disease-causing RPE gene, *VMD2*, showed a different topography of expression, with a relative deficiency state in the central versus the peripheral retina. RPE65, used as a control in that study, had properties consistent with our observations (31). Taken together, these observations suggest a potential role of both

RPE65-based and RPE65-independent pigment regeneration pathways in maintaining cone function and survival in primate maculas.

Our inquiry as to how *RPE65*-LCA alters the human retinal cone phenotype assumes that a state of RPE65 isomerase deficiency was present due to the homozygous or compound heterozygous mutations in our cohort of patients. *In vitro* assays of isomerase activity of *RPE65* mutations have indicated that most of these alleles have little or no activity (18, 32, 33). However, some of the mutants' activities have not been reported (see both alleles in P2, P3, P7, P12, and P23 and one allele in P17 and P19) (Table 1). Thus, possible explanations for residual central cone survival in humans, despite RPE65 isomerase deficiency, include partial activity of the mutant RPE65 enzyme, alternative pathways for chromophore regeneration, and resistance of human cones to degeneration even when the chromophore is not present.

Central cone photoreceptor layer abnormalities in the youngest patients studied (as early as age 3) suggest there is a human counterpart to the early and major cone photoreceptor loss noted in the first month of life for *Rpe65*$^{-/-}$ mice (34–37). However, macular cone photoreceptors in humans could persist for decades and show only a slow age-related decline. The present study suggests that RPE65 isomerase deficiency causes early cone loss, but does not answer the question of why a subset of cones survives this initial insult and undergoes a protracted phase of degeneration over ensuing decades. A partial supply of chromophore generated through hypomorphic alleles or alternative metabolic pathways could be sufficient to allow for the survival of a subset of cones. It also is possible that cones, which normally operate at much larger bleaching levels than rods, are more resistant to the chromophore deprivation. Thus, they may not degenerate with reduced or absent chromophore for an extended period. Slow degeneration of the cones may be caused by secondary RPE disease, leading to stressed photoreceptors already compromised by deficient chromophore (38, 39). Consistent with such a hypothesis, demelanization of the macular RPE became detectable in the third decade of life in *RPE65*-LCA patients. Other possibilities include changes in the structural and biochemical microenvironment, which are known to induce cone cell degeneration. These changes can be introduced by loss of structural support of neighboring rods due to lack of visual chromophore supplementation or alterations in the interphotoreceptor matrix that contains factors promoting cone survival (40).

What do the present results mean for *RPE65*-LCA patients being considered for clinical trials of gene therapy? Large animal studies to date, including primate safety studies, have mainly treated the area centralis or central retinal region (14, 41–43), so this region is a likely target for subretinal gene therapy. Thus, our finding of early foveal cone loss has strong clinical relevance. Expectations may need revision, but there is still hope that some useful cone photoreceptor-mediated central vision will be restored in this serious eye disease. Even a limited, partly functional central island of (cone) vision would be a boon for mobility and the tasks of everyday life (44).

Materials and Methods

Human Subjects. LCA patients with *RPE65* mutations ($n = 23$; ages 3–52 years) were included, and normal subjects ($n = 32$; ages 4–63 years) also were studied. All patients underwent a complete ophthalmic examination and visual function studies. Informed consent was obtained. Procedures followed the Declaration of Helsinki guidelines and were approved by the institutional review board.

OCT. Cross-sectional images of the central retina were acquired by OCT (Carl Zeiss Meditec, Dublin, CA). Principles of the method and our recording and analysis techniques have been published (45–50). Overlapping OCT scans of 4.5-mm lengths were used to cover horizontal and vertical meridians up to 9 mm eccentricity from the fovea. At least three OCTs were obtained at each retinal location. Two or three repeated scans were averaged to increase the signal-to-noise ratio and allow for better definition of retinal laminae. Postacquisition processing of OCT data was performed with custom programs (MATLAB 6.5; MathWorks, Natick, MA). Longitudinal reflectivity profiles making up the OCT scans were aligned by using a dynamic cross-correlation algorithm. Retinal thickness was defined as the distance between the signal transition at the vitreoretinal interface (labeled T1 in ref. 45) and the major signal peak corresponding to the RPE (48). In normal subjects, the RPE peak was assumed to be the last peak within the two- or three-peaked scattering signal complex (labeled ORCC in ref. 45) deep in the retina. In patients, the presumed RPE peak sometimes was the only signal peak deep in the retina, whereas other times it was apposed by other major peaks. In the latter case, the RPE peak was specified manually by considering the properties of the backscattering signal originating from layers vitread and sclerad to it. ONL thickness was defined as the major intraretinal signal trough delimited by the signal slope maxima and sampled every 0.15 mm as previously described (22). Average ONL thickness of the foveal region was defined based on the 17 samples forming a cross centered at the fovea and extending 0.6 mm along horizontal and vertical meridians.

Localized pigmentation of the RPE was estimated by calculating the sRBI, which was defined as the normalized partial integral of the backscattering signal over the retinal depth (48, 51). The partial integral was performed from the RPE signal peak toward the scleral direction and was divided by the signal intensity at the RPE peak to normalize for pre-RPE attenuation of light intensity. Average foveal sRBI was based on the 17 samples obtained every 0.15 mm and forming a cross centered at the fovea with 0.6-mm extensions. Under the assumption that RPE pigmentation is the dominant scatterer and absorber of near-infrared light, sRBI can be used as a measure of RPE disease associated with depigmentation (47, 48, 51).

Visual Thresholds and Fixation Stability. Dark-adapted chromatic thresholds were measured by using a modified automated perimeter (25, 52). SW-cone sensitivity measurements were made according to published methods (53). Techniques, methods of data analysis, and normal results have been described (25, 30, 47–49, 52).

Stability of fixation was determined by recording the retinal location of the anatomical fovea at video rate (MP1; Nidek, Fremont, CA) during a fixation task involving visualization of a red target; the length of recording was 45 sec. The fixation light was ≈3 log units brighter than normal perceptual threshold, and patients tested could see the target throughout the recording period. The movement of the retinal image with respect to fixation was recorded as horizontal and vertical offset values. A representative 10-sec epoch was selected, and the radial distance of all offsets from the centroid of the data set was calculated. The standard deviation of the radial distances was reported as a measure of fixation instability.

Animals. Eyes from cynomolgus (*Macaca fascicularis*) monkeys ($n = 12$; 6 female, 6 male; age 4 years) were collected under room light within 20 min of being killed and used for retinoid biochemical and immunohistochemical analyses. Studies were done in accordance with the Association for Research in Vision and Ophthalmology Statement for the Use of Animals in Ophthalmic and Vision Research and Institutional Review.

Immunohistochemistry. Eyes were fixed after enucleation, and the posterior segments were isolated, trimmed, and processed for embedding in an optimal cutting temperature medium as previously described (54). Ten-micrometer-thick cryosections through the fovea and extending 5,500 μm inferiorly and 10,000 μm superiorly were used for double-fluorescence immunohistochemistry (54). Primary antibodies used were: 1:10,000 dilution rabbit polyclonal anti-RPE65 (from T. M. Redmond, National Eye Institute, Bethesda, MD); 1:100 dilution goat polyclonal anti-human red/green

opsin (sc-22117; Santa Cruz Biotechnology, Santa Cruz, CA), 1:50 dilution goat polyclonal anti-human blue opsin (sc-14363; Santa Cruz Biotechnology), 1:1,000 dilution mouse monoclonal anti-rat rhodopsin (MAB5316; Chemicon, Temecula, CA), and 1:10,000 dilution rabbit polyclonal anti-human cone arrestin (from C. Craft, University of Southern California, Los Angeles, CA). Antigen–antibody complexes were visualized with fluorochrome-labeled secondary antibodies (Alexa Fluor, 1:200; Invitrogen, Carlsbad, CA). DAPI stain was used to detect cell nuclei. Slides were mounted and examined with an epifluorescence microscope (Axioplan; Carl Zeiss) equipped with Nomarski differential interference contrast optics. Negative control sections were treated identically but with omission of the primary antibodies.

Preparation of RPE Microsomes and Assay for Isomerase Activity. RPE was dissected from biopsies obtained from different regions of the eye by vigorous brushing with 25 mM Mops buffer (pH 7.0) containing 0.25 M sucrose and 1 mM DTT. Cell suspensions were homogenized and spun for 10 min at 8,000 $\times$ *g*. RPE membrane fractions were collected by ultracentrifugation at 120,000 $\times$ *g* for 1 h at 4°C and resuspended in 50 mM BTP buffer (pH 7.4). Commercially available antibody against RPE65 (Novus, Littleton, CO) was used to detect RPE65 expression levels by immunoblotting. The isomerization assay was performed in 25 mM BTP buffer (pH 7.4) in the presence of 1 mM ATP, 1% BSA, and 10 μM cellular retinaldehyde-binding protein. *All-trans*-retinol was used as a substrate at 10 μM concentration delivered in 0.8 μl of dimethylformamide. UV-treated RPE microsomes (100 μg of protein) were used as a source of enzymatic activity (55). The reaction was performed at 30°C for 80 min and then stopped by adding 300 μl of methanol followed by the same volume of hexane. Retinoids were extracted with hexane and analyzed on a Hewlett Packard 1100 series HPLC system equipped with a 5-μm, 4.5 $\times$ 250-mm column Agilent Si under isocratic elution conditions (10% ethyl acetate in hexane, 1.4 ml/min).

This work was supported in part by National Institutes of Health Grants EY017280, EY09339, and P30 EY11373, Macula Vision Research Foundation, Foundation Fighting Blindness, Hope for Vision, Macular Disease Foundation, Ruth and Milton Steinbach Fund, and Alcon Research Institute.

1. Arshavsky VY, LambTD, Pugh EN, Jr (2002) *Annu Rev Physiol* 64:153–187.
2. Lamb TD, Pugh EN, Jr (2004) *Prog Retin Eye Res* 23:307–380.
3. McBee JK, Palczewski K, Baehr W, Pepperberg DR (2001) *Prog Retin Eye Res* 20:469–529.
4. Palczewski K (2006) *Annu Rev Biochem* 75:743–767.
5. Travis GH, Golczak M, Moise AR, Palczewski K (2007) *Annu Rev Pharmacol Toxicol* 47:469–512.
6. Thompson DA, Gal A (2003) *Prog Retin Eye Res* 22:683–703.
7. Goldstein EB, Wolf BM (1973) *Vision Res* 13:527–534.
8. Hood DC, Hock PA (1973) *Vision Res* 13:1943–1951.
9. Mata NL, Radu RA, Clemmons RC, Travis GH (2002) *Neuron* 36:69–80.
10. Mata NL, Ruiz A, Radu RA, Bui TV, Travis GH (2005) *Biochemistry* 44:11715–11721.
11. Wenzel A, von Lintig J, Oberhauser V, Tanimoto N, Grimm C, Seeliger MW (2007) *Invest Ophthalmol Vis Sci* 48:534–542.
12. Znoiko SL, Crouch RK, Moiseyev G, Ma JX (2002) *Invest Ophthalmol Vis Sci* 43:1604–1609.
13. Hemati N, Feathers KL, Chrispell JD, Reed DM, Carlson TJ, Thompson DA (2005) *Mol Vis* 11:1151–1165.
14. Acland GM, Aguirre GD, Bennett J, Aleman TS, Cideciyan AV, Bennicelli J, Dejneka NS, Pearce-Kelling SE, Maguire AM, Palczewski K, *et al.* (2005) *Mol Ther* 12:1072–1082.
15. Redmond TM, Yu S, Lee E, Bok D, Hamasaki D, Chen N, Goletz P, Ma JX, Crouch RK, Pfeifer K (1998) *Nat Genet* 20:344–351.
16. Rando RR (2001) *Chem Rev* 101:1881–1896.
17. Jin M, Li S, Moghrabi WN, Sun H, Travis GH (2005) *Cell* 122:449–459.
18. Redmond TM, Poliakov E, Yu S, Tsai JY, Lu Z, Gentleman S (2005) *Proc Natl Acad Sci USA* 102:13658–13663.
19. Moiseyev G, Chen Y, Takahashi Y, Wu BX, Ma JX (2005) *Proc Natl Acad Sci USA* 102:12413–12418.
20. Curcio CA, Sloan KR, Kalina RE, Hendrickson AE (1990) *J Comp Neurol* 292:497–523.
21. Provis JM, Penfold PL, Cornish EE, Sanercoe TM, Madigan MC (2005) *Clin Exp Optom* 88:269–281.
22. Jacobson SG, Aleman TS, Cideciyan AV, Sumaroka A, Schwartz SB, Windsor EA, Traboulsi EI, Heon E, Pittler SJ, Milam AH, *et al.* (2005) *Proc Natl Acad Sci USA* 102:6177–6182.
23. Bainbridge JW, Tan MH, Ali RR (2006) *Gene Ther* 13:1191–1197.
24. Aguirre GK, Komaromy AM, Cideciyan AV, Brainard DH, Aleman TS, Roman AJ, Avants BB, Gee JC, Korczykowski M, Hauswirth WW, *et al.* (2007) *PLoS Med* 4:e230.
25. Jacobson SG, Voigt WJ, Parel JM, Apathy PP, Nghiem-Phu L, Myers SW, Patella VM (1986) *Ophthalmology* 93:1604–1611.
26. Paunescu K, Wabbels B, Preising MN, Lorenz B (2005) *Graefes Arch Clin Exp Ophthalmol* 243:417–426.
27. Putnam NM, Hofer HJ, Doble N, Chen L, Carroll J, Williams DR (2005) *J Vis* 5:632–639.
28. Alexander KR, Derlacki DJ, Fishman GA, Peachey NS (1991) *Invest Ophthalmol Vis Sci* 32:1446–1454.
29. Alexander KR, Derlacki DJ, Fishman GA (1995) *Vision Res* 35:1495–1499.
30. Cideciyan AV, Swider M, Aleman TS, Sumaroka A, Schwartz SB, Roman MI, Milam AH, Bennett J, Stone EM, Jacobson SG (2005) *Invest Ophthalmol Vis Sci* 46:4739–4746.
31. Mullins RF, Kuehn MH, Faidley EA, Syed NA, Stone EM (2007) *Invest Ophthalmol Vis Sci* 48:3372–3380.
32. Takahashi Y, Chen Y, Moiseyev G, Ma JX (2006) *J Biol Chem* 281:21820–21826.
33. Chen Y, Moiseyev G, Takahashi Y, Ma JX (2006) *FEBS Lett* 580:4200–4204.
34. Znoiko SL, Rohrer B, Lu K, Lohr HR, Crouch RK, Ma JX (2005) *Invest Ophthalmol Vis Sci* 46:1473–1479.
35. Bemelmans AP, Kostic C, Crippa SV, Hauswirth WW, Lem J, Munier FL, Seeliger MW, Wenzel A, Arsenijevic Y (2006) *PLoS Med* 3:e347.
36. Cottet S, Michaut L, Boisset G, Schlecht U, Gehring W, Schorderet DF (2006) *FASEB J* 20:2036–2049.
37. Chen Y, Moiseyev G, Takahashi Y, Ma JX (2006) *Invest Ophthalmol Vis Sci* 47:1177–1184.
38. Fan J, Woodruff ML, Cilluffo MC, Crouch RK, Fain GL (2005) *J Physiol* 568:83–95.
39. Woodruff ML, Wang Z, Chung HY, Redmond TM, Fain GL, Lem J (2003) *Nat Genet* 35:158–164.
40. Hewitt AT, Lindsey JD, Carbott D, Adler R (1990) *Exp Eye Res* 50:79–88.
41. LeMeur G, Weber M, Pereon Y, Mendes-Madeira A, Nivard D, Deschamps JY, Moullier P, Rolling F (2005) *Arch Ophthalmol* 123:500–506.
42. Jacobson SG, Acland GM, Aguirre GD, Aleman TS, Schwartz SB, Cideciyan AV, Zeiss CJ, Komaromy AM, Kaushal S, Roman AJ, *et al.* (2006) *Mol Ther* 13:1074–1084.
43. Jacobson SG, Boye SL, Aleman TS, Conlon TJ, Zeiss CJ, Roman AJ, Cideciyan AV, Schwartz SB, Komaromy AM, Doobrajh M, *et al.* (2006) *Hum Gene Ther* 17:845–858.
44. Szlyk JP, Seiple W, Fishman GA, Alexander KR, Grover S, Mahler CL (2001) *Ophthalmology* 108:65–75.
45. Huang Y, Cideciyan AV, Papastergiou GI, Banin E, Semple-Rowland SL, Milam AH, Jacobson SG (1998) *Invest Ophthalmol Vis Sci* 39:2405–2416.
46. Jacobson SG, Cideciyan AV, Aleman TS, Pianta MJ, Sumaroka A, Schwartz SB, Smilko EE, Milam AH, Sheffield VC, Stone EM (2003) *Hum Mol Genet* 12:1073–1078.
47. Cideciyan AV, Aleman TS, Swider M, Schwartz SB, Steinberg JD, Brucker AJ, Maguire AM, Bennett J, Stone EM, Jacobson SG (2004) *Hum Mol Genet* 13:525–534.
48. Jacobson SG, Cideciyan AV, Sumaroka A, Aleman TS, Schwartz SB, Windsor EA, Roman AJ, Stone EM, MacDonald IM (2006) *Invest Ophthalmol Vis Sci* 47:4113–4120.
49. Jacobson SG, Cideciyan AV, Aleman TS, Sumaroka A, Schwartz SB, Windsor EA, Roman AJ, Heon E, Stone EM, Thompson DA (2007) *Invest Ophthalmol Vis Sci* 48:332–338.
50. Cideciyan AV, Aleman TS, Jacobson SG, Khanna H, Sumaroka A, Aguirre GK, Schwartz SB, Windsor EA, He S, Chang B, *et al*. (June 6, 2007) *Hum Mutat*, 0.1002/humu.20565.
51. Cideciyan AV, Swider M, Aleman TS, Roman MI, Sumaroka A, Schwartz SB, Stone EM, Jacobson SG (2007) *J Opt Soc Am A* 24:1457–1467.
52. Roman AJ, Schwartz SB, Aleman TS, Cideciyan AV, Chico JD, Windsor EA, Gardner LM, Ying GS, Smilko EE, Maguire MG, Jacobson SG (2005) *Exp Eye Res* 80:259–272.
53. Jacobson SG, Marmor MF, Kemp CM, Knighton RW (1990) *Invest Ophthalmol Vis Sci* 31:827–838.
54. Beltran WA, Hammond P, Acland GM, Aguirre GD (2006) *Invest Ophthalmol Vis Sci* 47:1669–1681.
55. Stecher H, Gelb MH, Saari JC, Palczewski K (1999) *J Biol Chem* 274:8577–8585.
56. Lotery AJ, Namperumalsamy P, Jacobson SG, Weleber RG, Fishman GA, Musarella MA, Hoyt CS, Heon E, Levin A, Jan J, *et al.* (2000) *Arch Ophthalmol* 118:538–543.
57. Thompson DA, Gyurus P, Fleischer LL, Bingham EL, McHenry CL, Apfelstedt-Sylla E, Zrenner E, Lorenz B, Richards JE, Jacobson SG, *et al.* (2000) *Invest Ophthalmol Vis Sci* 41:4293–4299.
58. Thompson DA, McHenry CL, Li Y, Richards JE, Othman MI, Schwinger E, Vollrath D, Jacobson SG, Gal A (2002) *Am J Hum Genet* 70:224–229.